Nonlinear Resonances in the Attitude Motion of Dual-Spin Spacecraft

J.E. Cochran*
Auburn University, Auburn, Ala.

The attitude motion of a class of dual-spin spacecraft which exhibit nonlinear resonances during the despin process is studied. The model adopted consists of a rigid slightly asymmetric rotor and a rigid symmetric platform that is dynamically unbalanced with respect to the rotor's axis of maximum moment of inertia. No external torques are considered. Attitude equations are derived in an unconventional form that allows easy incorporation of the integral of angular momentum. The presence of a nonlinear resonance is shown to depend on the coexistence of rotor asymmetry and platform dynamic unbalance. An approximate solution for the attitude motion near resonance is obtained for the case of zero despin-motor torque by using the generalized method of averaging. The salient characteristics of the near-resonant motion are obtained from integrals of the averaged equations.

Nomenclature

$A=A_1$	=maximum centroidal moment of inertia of rotor
$a\equiv\sin\theta\equiv x_1$	=sine of spacecraft coning angle
A_1,A_2,A_3	=centroidal moments of inertia of rotor
B	$=A_2+B_2+D$
$\boldsymbol{B}$	=centroidal inertia tensor of platform
B_1,B_2,B_3	=centroidal moments of inertia of platform
C	$=A_3+B_3+D$; also used to denote center of mass of spacecraft
$CXYZ$	=nonrotating reference frame
$Cxyz$	=rotor-fixed reference frame aligned with $C_Ax_1x_2x_3$
$\boldsymbol{C}$	=rotation matrix relating platform and rotor bases
C_A	=center of mass of rotor
$C_Ax_1x_2x_3$	=rotor-fixed reference frame
C_B	=center of mass of platform
$C_By_1y_2y_3$	=platform-fixed reference frame
$cn\ u$	=Jacobian elliptic cosine function (cosine amplitude u).
$C\xi\eta\zeta$	=reference frame that lags the $Cxyz$ reference frame by the angle α
D	$=r^2m_Am_B/(m_A+m_B)$
$(\hat{e}_1,\hat{e}_2,\hat{e}_3)$	=rotor-fixed unit vector triad
$\boldsymbol{H}$	=rotational angular momentum of spacecraft
H	$=\lvert\boldsymbol{H}\rvert$, magnitude of rotational angular momentum of spacecraft
H_1,H_2,H_3	=x_1,x_2, and x_3 components, respectively, of $\boldsymbol{H}$ ($H_1=H\cos\theta$, $H_2=H\sin\theta\sin\phi$, $H_3=H\sin\theta\cos\phi$)
$\boldsymbol{I}$	=spacecraft centroidal inertia tensor
$\mathcal{K}$	=averaged value of approximate rotational kinetic energy
K	=complete elliptic integral of the first kind
k	=elliptic modulus
L	=inertia matrix associated with the change from the variable set $(\omega_1,\omega_2,\omega_3,\Omega,\alpha)$ to the set $(H_1,H_2,H_3,P_\alpha,\alpha)$
L_1,L_2,L_3	=averaged, normalized ξ, η and ζ components, respectively, of $\boldsymbol{H}$ ($L_1=\cos\theta$, $L_2=\sin\theta\sin\bar{y}_1$, $L_3=\sin\theta\cos\bar{y}_1$)
m_A	=mass of rotor
m_B	=mass of platform
P	=platform product of inertia
P_α	=momentum conjugate to α (physically, the x_1 component of the rotational angular momentum of the platform)
p_α	$\equiv P_\alpha/H\equiv x_2$, normalized values of P_α
r	=distance between centers of mass of rotor and platform
$sn\ u$	=Jacobian elliptic sine function (sine amplitude u)
$\boldsymbol{T}$	$=T_\alpha\hat{e}_1$, internal torque generated by despin motor
$\mathfrak{I}$	=rotational kinetic energy of spacecraft
t	=time
u	$=\lambda(\tau-\tau_0)$, argument of Jacobian elliptic functions
X_i	=M vector of periodic functions
$\boldsymbol{x}$	=M vector of slow variables
x_1	$\equiv a\equiv\sin\theta$
x_2	$=p_\alpha\equiv P_\alpha/H$
Y_0	=N vector of unperturbed angular rates
Y_i	=N vector of periodic functions
$\boldsymbol{y}$	=N vector of fast variables
y_1	$\equiv\phi-\alpha$
y_2	$\equiv\phi+\alpha$
α	=angle of relative rotation of platform with respect to rotor
δ	=small parameter
ϵ	$\equiv P/B_1$, treated as a small parameter
Λ_α	=approximation to $(A/H)\Omega$
Λ_ϕ	=approximation to $(A/H)\omega_\phi$
λ	=frequency of Jacobian elliptic functions
μ	$\equiv(B-C)/B$, asymmetry parameter
Ω	=spin rate of platform with respect to rotor
ω	=angular velocity of rotor
$\omega_1,\omega_2,\omega_3$	=x_1,x_2, and x_3 components of ω
ω_ϕ	=absolute value of nonperiodic part of $\dot{\phi}$
ϕ	=spin angle of rotor
ψ	=precession angle of the rotor-fixed $Cxyz$ reference frame
θ	=coning angle of spacecraft
τ	$\equiv(H/A)t$

Superscripts

$\bar{(\ )}$	=average value of ( )
$(\dot{})$	=time rate of change of the elements only of the matrix ( )

Presented as Paper 76-787 at the AIAA/AAS Astrodynamics Conference, San Diego, Calif., Aug. 18-20, 1976; submitted Nov. 12, 1976; revision received April 20, 1977.
Index category: Spacecraft Dynamics and Control.
*Associate Professor, Aerospace Engineering. Member AIAA.

$(\dot{})$ = time rate of change of the scaler ( )
$(\,)'$ = d( )/dτ
$(\,)^T$ = transpose of the matrix ( )

Subscripts

$(_P)$ = vector of tensor quantity ( ) expressed in the platform basis
$(_r)$ = vector or tensor quantity ( ) expressed in the rotor basis
$(\,)_r$ = resonance value

I. Introduction

NONLINEAR resonance is an interesting, and often troublesome, phenomenon that may be observed in the motions of many types of nonlinear dynamical systems. Some examples are a simple pendulum subjected to a sinusoidally time-varying torque; two coupled pendulums; a synchronous, artificial Earth satellite;[1] a rigid body rotating about its center of mass which is moving in an inverse square gravity field[2]; and a dual-spin spacecraft with axisymmetric platform and rotor, each of which contains an elastically constrained point-mass "nutation damper."[3]

Unless it is known a priori that the possible states of a dynamical system include motion near a nonlinear resonance, significant problems may arise because, depending on the nature of the resonance, rather violent "oscillations" may occur. This is especially true if energy is being added to the system, as Scher and Farrenkopf[4] discovered in a study of the type of dual-spin spacecraft considered in this paper.

The authors of Ref. 4 investigated the dynamical behavior of a dual-spin spacecraft model that consisted of an asymmetric rigid rotor, an axially symmetric but dynamically unbalanced (with respect to the bearing axis) platform, and a low-torque electric motor for despinning the platform. By numerically integrating the equations of motion, they studied the externally torque-free attitude motions of this system during the despin process, beginning with the state corresponding to minimum energy, and discovered two types of "dynamic trap states." One of these is the "minimum energy trap," which is difficult to "escape" from if the despin motor has very limited torque capabilities. The second type consists of "resonance trap states" in which the energy added by the motor goes not into despinning the platform but rather into producing a larger mean coning angle and progressively more violent oscillations of this angle about its mean value (nutation). In Ref. 4, the authors presented a heuristic explanation of the "resonance trap" and commented that better understanding of such motion is needed. The purpose of this paper is to present an analysis of this nonlinear resonance problem.

In this paper, the model used in Ref. 4 is adopted, and equations of motion are derived in terms of rather nonconventional variables: the rotor-fixed components of the total rotational angular momentum of the spacecraft, the momentum conjugate† to the angle of rotation of the platform relative to the rotor, and the angle of relative rotation. Approximate equations for these variables are obtained through first order in the ratio of the product of inertia of the platform and its momentum of inertia about its symmetry axis. This approach is akin to that used by Pringle[3] and Cochran[5] in analyzing satellite rotation-vibration problems. Here, however, canonical transformation theory is not used.

The five approximate equations first are reduced to a fourth-order set using the integral of angular momentum and then transformed into the normal form required by the method of averaging.[6-8] The existence of a nonlinear resonance when $|\Omega|$, the magnitude of the relative spin rate of the platform, is equal to ω_ϕ, the mean spin rate of a rotor-fixed coordinate frame, is apparent from the equations.‡ The possibility (under normal conditions) of a resonance does not exist when the rotor is symmetric or when the platform is dynamically balanced. A condition that the momentum conjugate to the angle of relative rotation of the platform and the cosine of the coning angle must satisfy at resonance is developed.

An approximate solution of the normal-form equations iso btained for motion near resonance by using the method of averaging. For the case of no motor torque, it is shown that $\cos\theta$, the "average" of the cosine of the coning angle, is a function of Jacobian elliptic functions. The "resonance trap" phenomenon is explained using integrals of the motion obtained for the case of zero motor torque and verified by numerical results.

II. Spacecraft Model

The model adopted for the present study is shown schematically in Fig. 1. It consists of a rigid, asymmetric (triaxial) rotor, denoted body A, and a rigid, axially symmetric§ platform, denoted body B. The platform has its axis of symmetry aligned with the bearing axis (x_1 axis) of the sytem but is assumed to be dynamically unbalanced with respect to that axis. The centers of mass of bodies A and B are C_A and C_B, respectively.

Two dextral, orthogonal coordinate systems are adopted (see Fig. 1). The $C_A x_1 x_2 x_3$ system [unit vector trihedral ($\hat{e}_1$, $\hat{e}_2$,$\hat{e}_3$)] is fixed in the rotor, and its axes are centroidal principal axes of that body. Similarly, the $C_B y_1 y_2 y_3$ system is fixed in the platform, but only y_2 is a principal axis of the platform. The distance between C_A and C_B is r, and m_A and m_B are the masses of the rotor and platform, respectively. The relative angle of rotation of body B with respect to body A is α. Also, C is the center of mass of the system of two bodies.

The centroidal inertia tensor for the system referred to axes parallel to those of the $C_A x_1 x_2 x_3$ system is¶

$$I = \begin{bmatrix} A_1+B_1 & -P\mathrm{s}\alpha & P\mathrm{c}\alpha \\ -P\mathrm{s}\alpha & A_2+B_3+D & 0 \\ P\mathrm{c}\alpha & 0 & A_3+B_3+D \end{bmatrix} \quad (1)$$

where A_j is the moment of inertia of body A about x_j, B_j is the moment of inertia of body B about y_j, $-P$ is the platform's product of inertia in the $x_1 y_3$ plane, and $D = r^2 m_A m_B/(m_A+m_B)$. To complete the model, an internal torque, $T = T_\alpha \hat{e}_1$, is assumed to be applied by the rotor to the platform, when it is so desired. The main purpose of this torque is, of course, to despin the platform.

III. Equations of Motion

Usually, the variables chosen for studying the motion of dynamical systems of the type considered here would be the angular velocity components of the rotor, the relative angular velocity of the platform, and the angle α. However, since the total angular momentum of the system about C is constant, we chose instead to use the $\hat{e}_j$ components of angular momentum of the system, the momentum conjugate to the angle α, and that angle as our variables. This complicates the derivation of equations of motion somewhat, but the resulting equations are particularly well suited for later transformation

†Physically, this momentum is the bearing axis component of the angular momentum of the platform.

‡The nutation frequency of the free gyrostat composed of an asymmetric rigid body and an axially symmetric rigid body is approximately $2\omega_\phi$ for small nutation angles.

§The platform is not axially symmetric in the strict sense, but, since $B_2 = B_3$, we shall refer to it as such.

¶We define $c(\,) \equiv \cos(\,)$ and $s(\,) \equiv \sin(\,)$ for convenience.

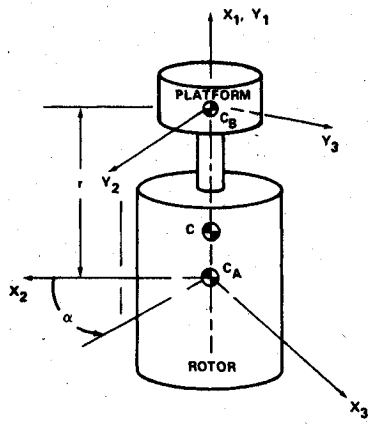

Fig. 1 Spacecraft model.

into the normal form needed for the application of the method of averaging.

The angular momentum of the system about C in the rotor basis is

$$\underset{r}{H}=\underset{rr}{I}\underset{r}{\omega}+\underset{pp}{C^T}\underset{p}{B}\underset{p}{\Omega} \tag{2}$$

where $H=[H_1\ H_2\ H_3]^T$, the letters r and p denote rotor and platform bases, respectively, $\omega=[\omega_1\ \omega_2\ \omega_3]^T$,

$$C^T=\begin{bmatrix}1 & 0 & 0\\ 0 & c\alpha & -s\alpha\\ 0 & s\alpha & c\alpha\end{bmatrix} \tag{3}$$

$$B_p=\begin{bmatrix}B_1 & 0 & P\\ 0 & B_3 & 0\\ P & 0 & B_3\end{bmatrix} \tag{4}$$

and $\Omega=[\Omega\ 0\ 0]^T$ (the relative angular velocity of the platform). Also, the kinetic energy of the system due to rotation about C is

$$\mathfrak{I}=\tfrac{1}{2}[\omega^T I\omega+2\Omega^T BC\omega+\Omega^T B\Omega] \tag{5}$$

Since $\dot{\alpha}=\Omega$, P_α, the momentum conjugate to α, may be expressed as

$$P_\alpha=\frac{\partial T}{\partial\Omega}=[1\ 0\ 0][B\ C\ \omega+B\Omega]$$

or

$$P_\alpha=B_1\omega_1+P[-\omega_2 s\alpha+\omega_3 c\alpha]+B_1\Omega \tag{6}$$

Physically, P_α is the x_1 component of the angular momentum of the platform. We note that, if $\Omega=-\omega_1$ and $\omega_2=\omega_3=0$, or $P=0$, then $P_\alpha=0$. Equation (6) may be rearranged to obtain

$$\dot{\alpha}=P_\alpha/B_1-\omega_1-(P/B_1)[-\omega_2 s\alpha+\omega_3 c\alpha] \tag{7}$$

and, by using Eq. (7) to rewrite Eq. (2) in terms of the ω_j, α, and P_α and then solving for ω, we obtain

$$\omega=L^{-1}(H-h_\alpha) \tag{8}$$

where

$$L=\begin{bmatrix}A_1 & 0 & 0\\ 0 & A_2+B_3-(P^2/B_1)s^2\alpha+D & [P^2/(2B_1)]s2\alpha\\ 0 & [P^2/(2B_1)]s2\alpha & A_3+B_3-(P^2/B_1)c^2\alpha+D\end{bmatrix} \tag{9}$$

and

$$h_\alpha=P_\alpha\begin{bmatrix}1\\ -(P/B_1)s\alpha\\ (P/B_1)c\alpha\end{bmatrix} \tag{10}$$

Because the rotational motion of the system is torque-free,

$$\mathring{H}=[\dot{H}_1\dot{H}_2\dot{H}_3]^T=\tilde{H}\omega \tag{11}$$

where

$$\tilde{H}=\begin{bmatrix}0 & -H_3 & H_2\\ H_3 & 0 & -H_1\\ -H_2 & H_1 & 0\end{bmatrix} \tag{12}$$

is the matrix counterpart of the vector operation $H\times$. We now may use Eqs. (8) and (11) to write

$$\mathring{H}=\tilde{H}L^{-1}(H-h_\alpha) \tag{13}$$

Equations (7) and (13) are exact, since no approximations have been introduced, and they represent four of the five equations required to determine the motion of the system (except for the precession of the x axis). The remaining equation is for P_α. This equation may be obtained by writing the expression for the angular momentum of B about its center of mass in the matrix form

$$\underset{p}{H_B}=\begin{bmatrix}P_\alpha\\ B_3[\omega_2 c\alpha+\omega_3 s\alpha]\\ P(\omega_1+\Omega)+B_3[-\omega_2 s\alpha+\omega_3 c\alpha]\end{bmatrix} \tag{14}$$

and computing the derivative of the vector H_B. Hence,

$$\underset{p}{\mathring{H}_B}=-\underset{pp}{\tilde{\omega}}\underset{p}{H_B}+[T_\alpha\ 0\ 0]^T+[0\ T_{2c}\ T_{3c}]^T \tag{15}$$

where $\underset{p}{\omega}=\underset{r}{C\omega}$, and T_{2c} and T_{3c} are constraint torque components. Because $B_2=B_3$, we get for P_α the differential equation

$$\dot{P}_\alpha=-P(\omega_1+\Omega)(\omega_2 c\alpha+\omega_3 s\alpha)+T_\alpha \tag{16}$$

where the ω_j may be replaced by functions of H_k, α, and P_α using Eq. (8).

In the sequel, we also shall need the kinetic energy due to rotation of the system about C, expressed in our choice of variables. By starting with Eq. (5) and using Eq. (6) and Eq. (8), we obtain, after considerable simplification,

$$\mathfrak{I}=\tfrac{1}{2}(H-h_\alpha)^T L^{-1}(H-h_\alpha)+\tfrac{1}{2}P_\alpha^2/B_1 \tag{17}$$

IV. Approximate Equations, Normal-Form Equations, and Resonance Conditions

Approximate Equations

To determine qualitatively the effects of the platform's "small" product of inertia on the system's motion, it is necessary that we retain only the terms in Eqs. (8, 13, and 16) which are zeroth or first order in $\epsilon=P/B_1$. This requires the computation of the inverse of L through first order in P/B_1.

Hence, we may use**

$$L^{-1} \simeq \begin{bmatrix} 1/A & 0 & 0 \\ 0 & 1/B & 0 \\ 0 & 0 & 1/C \end{bmatrix} \tag{18}$$

where $A=A_1$, $B=A_2+B_3+D$, and $C=A_3+B_3+D$. The terms that are first order in P/B_1 are contained in P_α and h_α.

To the stated order of approximation, we get

$$\omega_1 \simeq H_1/A - P_\alpha/A \tag{19a}$$

$$\omega_2 \simeq H_2/B + \epsilon(P_\alpha/B)s\alpha \tag{19b}$$

$$\omega_3 \simeq H_3 C - \epsilon(P_\alpha/C)c\alpha \tag{19c}$$

It is then a simple matter to obtain

$$\dot{H}_1 \simeq [(B-C)/(BC)]H_2H_3 - \epsilon P_\alpha[CH_3s\alpha + BH_2c\alpha]/(BC) \tag{20a}$$

$$\dot{H}_2 \simeq [(C-A)/(AC)]H_1H_3 - H_3P_\alpha/A + \epsilon H_1(P_\alpha/C)c\alpha \tag{20b}$$

$$\dot{H}_3 \simeq [(A-B)/(AB)]H_1H_2 + H_2P_\alpha/A + \epsilon H_1(P_\alpha/B)s\alpha \tag{20c}$$

for the H_j. We also obtain

$$\dot{\alpha} \simeq (1/B_1 + 1/A)P_\alpha - H_1/A + \epsilon[CH_2s\alpha - BH_3c\alpha]/(BC) \tag{21a}$$

$$\dot{P}_\alpha \simeq -\epsilon P_\alpha[CH_2c\alpha + BH_3s\alpha]/(BC) + T_\alpha \tag{21b}$$

Note that no assumption as to the magnitude of the triaxiality of the rotor yet has been made.

Normal-Form Equations

To apply the method of averaging, we need equations of the form

$$\dot{x} = \delta X_1 + \delta^2 X_2 + \ldots \tag{22a}$$

$$\dot{y} = Y_0 + \delta Y_1 + \delta^2 Y_2 + \ldots \tag{22b}$$

where δ is a "small" constant, x is an M vector of slow variables, y is an N vector of fast variables, and the vector functions X_j and Y_k are periodic functions in the elements of y with period 2π.

To put Eqs. (20) and (21) into normal form, we first use the fact that the magnitude of the angular momentum of the system about C is constant. Hence,

$$H_1^2 + H_2^2 + H_3^2 = H^2, \text{ const} \tag{23}$$

and, since H_1 will be positive for the cases considered herein,

$$H_1 = \sqrt{H^2 - H_2^2 - H_3^2} \tag{24}$$

Thus, we need to consider only Eqs. (20b, 20c, and 21).

Next, we observe that, since the direction of H is fixed, the Euler angles Ψ, θ, and ϕ (see Fig. 2) may be used in a 1-2-1 sequence of rotations to specify the orientation of the $Cxyz$ system relative to a nonrotating system $CXYZ$, which has its X axis aligned with H. Thus, we may express H_2 and H_3 in the forms

$$H_2 = H\sin\theta\sin\phi \tag{25a}$$

$$H_3 = H\sin\theta\cos\phi \tag{25b}$$

**Note that P appears in L only in the combination P^2/B_1, which is second order.

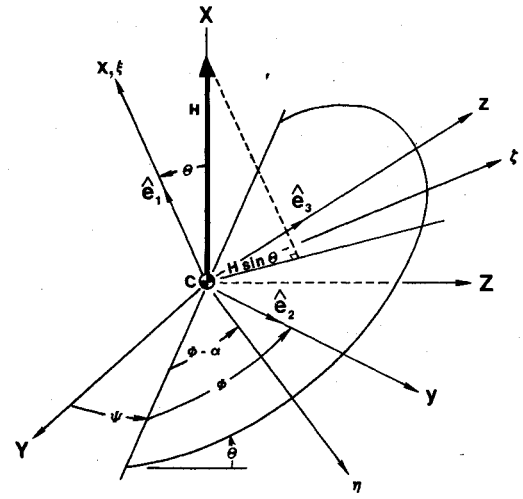

Fig. 2 Euler angles.

It follows from Eqs. (23) and (25) that we may use $\sin\theta$ and ϕ as variables instead of H_2 and H_3. Furthermore, from results for the motion of a single almost axisymmetric rigid body and of a gyrostat (Ref. 9, pp. 21-24, 207-238), we expect that ϕ will be a "fast" variable and θ will be a "slow" variable. Here "fast" implies that ϕ is monotonic even if $\epsilon=0$, whereas "slow" implies that θ, the coning angle, is bounded if $\epsilon=0$. In particular, if $\epsilon=0$ and $B=C$, θ is constant.

We let $a=\sin\theta$ and, for convenience, define $\tau \equiv (H/A)t$, $(\,)' \equiv d(\,)/d\tau$, $p_\alpha \equiv P_\alpha/H$, and $\mu \equiv (B-C)/B$. Then, using Eqs. (25) as transformation equations, we obtain

$$\begin{aligned} a' = {} & \mu[A/(2C)]a\sqrt{1-a^2}\sin 2\phi \\ & + \epsilon(2-\mu)[A/(2C)]p_\alpha\sqrt{1-a^2}\sin(\phi+\alpha) \\ & + \epsilon\mu[A/(2C)]p_\alpha\sqrt{1-a^2}\sin(\phi-\alpha) \end{aligned} \tag{26a}$$

$$\begin{aligned} \phi' = {} & -\Lambda_\phi - \mu[A/(2C)]\sqrt{1-a^2}\cos 2\phi \\ & + \epsilon(2-\mu)[A/(2C)](p_\alpha/a)\sqrt{1-a^2}\cos(\phi+\alpha) \\ & + \epsilon\mu[A/(2C)](p_\alpha/a)\sqrt{1-a^2}\cos(\phi-\alpha) \end{aligned} \tag{26b}$$

where $\Lambda_\phi = \tfrac{1}{2}[A/C + A/B - 2]\sqrt{1-a^2} + p_\alpha$.

Using our new independent variable τ and the definitions just noted, we also get the following equations for p_α and α:

$$\begin{aligned} p_\alpha' = {} & -\epsilon(2-\mu)[A/(2C)]p_\alpha a\sin(\phi+\alpha) \\ & + \epsilon\mu[A/(2C)]p_\alpha a\sin(\phi-\alpha) + AT_\alpha/H^2 \end{aligned} \tag{26c}$$

$$\begin{aligned} \alpha' = {} & -\Lambda_\alpha - \epsilon(2-\mu)[A/(2C)]a\cos(\phi+\alpha) \\ & - \epsilon\mu[A/(2C)]a\cos(\phi-\alpha) \end{aligned} \tag{26d}$$

where $\Lambda_\alpha = -[(A+B_1)/B_1]p_\alpha + \sqrt{1-a^2}$.

Provided that μ is as small as α and that AT_α/H^2 also is small, Eqs. (26) are in the proper form for applying the method of averaging. The slow variables are a and p_α, whereas ϕ and α are fast variables. The apparently awkward decomposition of Eqs. (26) has the purpose of grouping terms that contain trigonometric functions with the arguments 2ϕ, $\phi+\alpha$, and $\phi-\alpha$.

The distinction between $\dot{\phi}$, the rate at which the rotor spins about the x axis, and $\omega_1 = \dot{\phi} + \dot{\psi}\cos\theta$, the x component of the angular velocity of the rotor, must be understood clearly before the significance of certain terms in Eqs. (26) can be appreciated. For $A>B$, or C, $P_\alpha>0$, $\omega_1>0$, and $\epsilon=0$, $\dot{\phi}$ is negative, even though ω_1 is positive. For $\epsilon\neq 0$ but small, this

also is the case. The motion is such that the entire spacecraft precesses about H at a rate $\dot{\psi} > \omega_l$, whereas the rotor spins about the x axis at a rate $\dot{\phi}$ and the platform spins about the x axis at a rate $\dot{\phi}+\dot{\alpha}$. Since $\dot{\alpha}=\Omega$ is zero in the "spun-up" state, $\dot{\alpha}$ will be equal to $\dot{\phi}$ at some time during despin unless $\dot{\phi}$ is less than the value of ω_l when the platform is despun. When $\dot{\phi} \simeq \dot{\alpha}$, the terms in Eq. (26) which contain the argument $\phi-\alpha$ will change slowly with time. Such motion is near-resonant motion.[1]

Resonance Conditions

In treating nonlinear resonance problems, characterized by equations of the form (26), exact resonance[1] is said to exist when the nonperiodic parts of the fast variables are commensurable. Here, the commensurability is between Λ_ϕ and Λ_α and is one of the first order. For $A>B$ and relatively small values of P_α, both Λ_ϕ and Λ_α are positive. Hence, exact resonance exists when $\Lambda_\phi = \Lambda_\alpha$. Letting a subscript r denote the value of a variable at resonance, we may express the condition $\Lambda_\phi = \Lambda_\alpha$ as

$$\sqrt{1-a_r^2} = 2[(A/B_l+2)/(4-A/B-A/C)]p_{\alpha_r} \quad (27)$$

Since $\cos\theta = \sqrt{1-a^2}$, Eq. (27) provides the relationship between the coning angle and the corresponding value of P_α which must exist at resonance.

It is also of interest to express the resonance condition in terms of ω_{lr} and Ω_r. Neglecting terms of order ϵ which are periodic in α,

$$\sqrt{1-a_r^2} \simeq [(A+B_l)\omega_{lr} - B_l\Omega_r]/H \quad (28a)$$

and, from Eq. (6).

$$P_{\alpha_r} \simeq B_l(\omega_{lr}+\Omega_r) \quad (28b)$$

It follows from Eqs. (27) and (28) that

$$\omega_{lr} \simeq -\gamma\Omega_r \quad (29)$$

where

$$\gamma = [2BC+B_l(B+C)]/[(A+B_l)(B+C)-2BC] \quad (30)$$

i.e., ω_{lr} and Ω_r are related in a linear manner. A representative resonance line is shown in Fig. 3.

The numerical values $A=300$ slug-ft^2, $B=250$ slug-ft^2, $C=275$ slug-ft^2, and $B_l=50$ slug-ft^2 correspond to physical characteristics of the spacecraft model studied in Ref. 4. Using these values, we obtain $\omega_{lr} \simeq -3.541\,\Omega_r$. For $\omega_{lr}=5.3$ rad/sec, the value of ω_l at which the simulation results of Ref. 4 indicate the existence of "resonant" motion, we get $\Omega_r \simeq -1.497$ rad/sec. This result agrees very well with the results of Ref. 4 and additional numerical integrations of the exact equations of motion.

Note that, if the slope of the line ω_{lr} vs $-\Omega_r$ is less than unity, despin can be accomplished without passing through the type of resonance considered here, since the resonance line lies to the right of the despun line. This slope is given by Eq. (30), and for $A>4BC/(B+C)$, $\gamma<1$. This result also follows from Eq. (27), since negative values of P_{α_r} are required if $A>4BC/(B+C)$. The question of whether the criterion $A>4BC/(B+C)$ may be satisfied by any physically realizable configuration naturally arises. Since $A=A_l$ must be less than A_2+A_3, physical realizability requires that $(2-\mu)-2(B_2+D)/B>A/B$. In Fig. 4, the curves $A/B=(2-\mu)-2(B_2+D)/B$ and $A/B=4(1-\mu)/(2-\mu)$ and the lines $A/B=1$ and $A/B=1-\mu/2$ (the line $A/B=-\mu/2$ corresponds to $A=[B+C]/2$ are shown for $2(B_2+D)/B=0.2$ For $\mu>0$ (that is, $B>C$), values of A/B and μ which lie within the shaded region satisfy both the criteria for physical realizability and $A>B>C$, and the criterion for $\gamma<1$ also is satisfied. Obviously, for the value of $2(B_2+D)/B$ used to construct Fig. 4, a satellite that satisfies all of the requirements will be very asymmetric.

V. Some Geometric Results

Before we turn to the task of obtaining approximate solutions to Eqs. (26), let us consider some geometric aspects of the motion of the spacecraft. The rotational kinetic energy of the spacecraft may be expressed approximately as

$$\mathfrak{I} \simeq \tfrac{1}{2}[(H_l-P_\alpha)^2/A + (H_2+\epsilon P_\alpha s\alpha)^2/B + (H_3-\epsilon P_\alpha c\alpha)^2/C + P_\alpha^2/B_l] \quad (31)$$

Considering P_α and α as "parameters" and the H_j as coordinates, Eq. (31) defines a family of ellipsoids whose origins are located at $(P_\alpha, -\epsilon P_\alpha s\alpha, \epsilon P_\alpha c\alpha)$ and whose axes are of lengths $(2\mathfrak{I}-P_\alpha/B_l)$ times A, B, and C. Also, Eq. (23) represents a family of spheres, each with origin (0, 0, 0). For a given set of initial conditions, a particular sphere of constant radius H is defined by Eq. (23), and if at any instant of time $\mathfrak{I}, P_\alpha$, and α are known, Eq. (31) defines a particular ellipsoid. Since H_j must be such that they satisfy both Eqs. (23) and

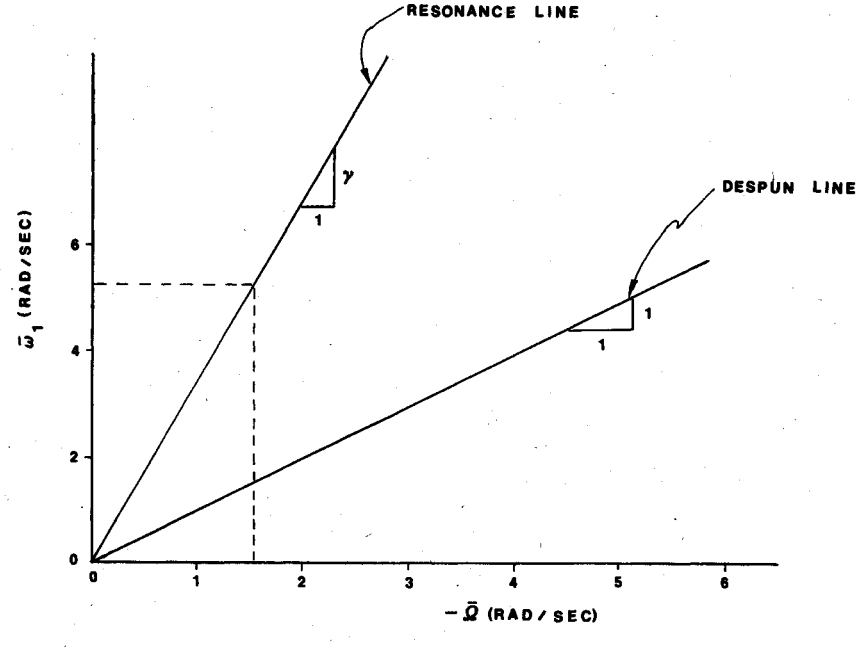

Fig. 3 Representative resonance line.

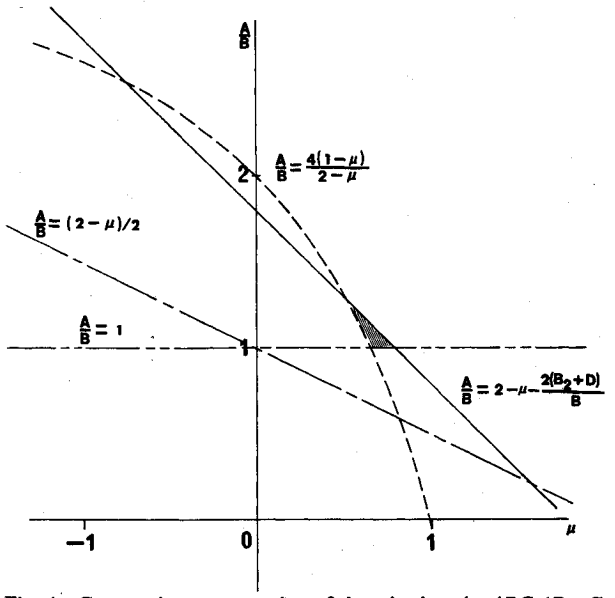

Fig. 4 Geometric representation of the criterion $A>4BC/(B+C)$.

(31), the terminus of the rotational angular momentum vector H lines on an intersection †† of the sphere and the "instantaneous" ellipsoid. As Eqs. (26) indicate, for motion far from resonance, we can consider α to be an essentially linear function of time and P_α to be approximately constant over a short period of time, say, one or two periods of $\sin\alpha$. Thus, for $\alpha=2n\pi$, the projection of the intersection of the ellipsoid and the sphere onto the H_2H_3 plane will appear as, say, curve 1 shown in Fig. 5 whereas for $\alpha=2n\pi+\pi/2$, $\alpha=2n\pi+\pi$, and $\alpha=2n\pi+3\pi/2$, respectively, the intersections will appear as curves 2, 3, and 4.

Now, $H_2=Hs\theta s\phi$ and $H_3=Hs\theta c\phi$, and, since ϕ is essentially a linear function of time, we can consider, to a good approximation (which becomes increasingly better as ϵ and $\mu\to0$), that the motion of the projection of the terminus of H onto the H_2H_3 plane lies on curves, 1, 2, 3, and 4 at, say, points a, b, c, and d as ϕ and α vary. Motion of this type has been obtained via numerical integration of the exact equations of motion.

Near resonance, with $T_\alpha=0$, P_α varies slowly and almost periodically with a relatively large amplitude. Thus, the center of the ellipsoid spirals outward from the H_1 axis, while simultaneously moving parallel to that axis. As a result of this motion, the projection of the curve of intersection on the H_2H_3 plane varies slowly and almost periodically in size. Resonant motion therefore may be interpreted as motion in which the variations in the "size" of the curve of intersection occur at the same frequency as the motion of the terminus of H along the curve. The associated amplitude variations in the coning angle may be either large or small depending on the location of the terminus of H on the curve of intersection when the curve is "largest." For example, if the terminus of H is on the part of the curve nearest the H_1 axis when the curve has its maximum "size" and on the part farthest from the H_1 axis when the "size" of the curve is a minimum, then "mostly fast-period" oscillations in θ will be observed.

If T_α is not zero, the "energy ellipsoid" grows larger if $2\mathfrak{I}-P_\alpha^2/B_1$ increases and smaller if the same quantity decreases. The particular choice depends on the functional form of T_α and its magnitude.

VI. Near-Resonant Motions

For motions in which the resonance condition $\Lambda_\phi=\Lambda_\alpha$ is approximately satisfied, the argument $\phi-\alpha$ is varying slowly, and the terms in Eqs. (26) which contain trigonometric

††There may, of course, be two intersections.

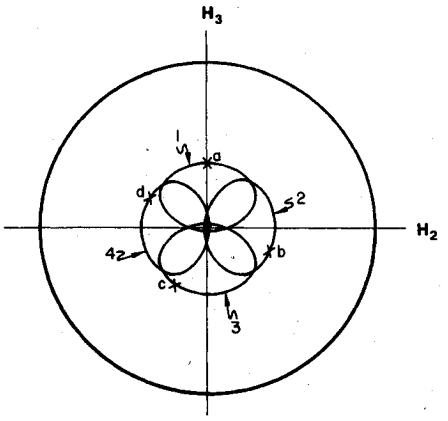

Fig. 5 Motion of the terminus of H.

functions with this argument constitute first-order, rather than second-order, effects. The other $\epsilon\mu$ terms may be neglected, since $\phi+\alpha$ is varying rapidly.

To analyze the near-resonant motions, we first define $x_1\equiv a$, $x_2\equiv p_\alpha$, $y_1\equiv\phi-\alpha$, and $y_2\equiv\phi+\alpha$. Then, by applying the averaging algorithm given in the Appendix, we get the averaged equations

$$\bar{x}_1'=\epsilon\mu[A/(2C)]\bar{x}_2\sqrt{1-\bar{x}_1^2}\sin\bar{y}_1 \tag{32a}$$

$$\bar{x}_2'=\epsilon\mu[A/(2C)]\bar{x}_1\bar{x}_2\sin\bar{y}_1+A\bar{T}_\alpha/H^2 \tag{32b}$$

$$\bar{y}_1'=-[\bar{\Lambda}_\phi(\bar{x}_1,\bar{x}_2)-\bar{\Lambda}_\alpha(\bar{x}_1,\bar{x}_2)]+\epsilon\mu[A/(2C)][(\bar{x}_2/\bar{x}_1)\sqrt{1-\bar{x}_1^2}+\bar{x}_1]\cos\bar{y}_1 \tag{32c}$$

$$\bar{y}_2'=-[\bar{\Lambda}_\phi+\bar{\Lambda}_\alpha]+\epsilon\mu[A/(2C)][(\bar{x}_1/\bar{x}_2)\sqrt{1-x_1^2}-\bar{x}_1]\cos\bar{y}_1 \tag{32d}$$

Also, dropping the small, second-order, short-period $\epsilon\mu$ terms, we obtain the transformation equations

$$a=\bar{x}_1+\mu b_1\cos(\bar{y}_1+\bar{y}_2)+\epsilon b_2\cos\bar{y}_2 \tag{33a}$$

$$p_\alpha=\bar{x}_2+\epsilon b_3\cos\bar{y}_2+\text{periodic terms due to } T_\alpha \tag{33b}$$

$$\phi=\tfrac{1}{2}[\bar{y}_1+\bar{y}_2]+\mu b_4\sin(\bar{y}_1+\bar{y}_2)+\epsilon b_5\sin y_2 \tag{33c}$$

$$\alpha=\tfrac{1}{2}[\bar{y}_2-\bar{y}_2]+\mu b_6\sin(\bar{y}_1+\bar{y}_2)+\epsilon b_7\sin\bar{y}_2 \tag{33d}$$

$$b_1=(A/C)\bar{x}_1\sqrt{1-x_1^2}/(4\bar{\Lambda}_\phi)$$

$$b_2=(A/C)\bar{x}_2\sqrt{1-x_1^2}/(\bar{\Lambda}_\phi+\bar{\Lambda}_\alpha)$$

$$b_3=-(A/C)\bar{x}_1\bar{x}_2/(\bar{\Lambda}_\phi+\bar{\Lambda}_\alpha)$$

$$b_4=b_1/\bar{x}_1+(\partial\bar{\Lambda}_\phi/\partial\bar{x}_1)b_1/(2\bar{\Lambda}_\phi)$$

$$b_5=b_2/\bar{x}_1+[(\partial\bar{\Lambda}_\phi/\partial\bar{x}_1)b_2+(\partial\bar{\Lambda}_\phi/\partial\bar{x}_2)b_3]/(\bar{\Lambda}_\phi+\bar{\Lambda}_\alpha)$$

$$b_6=-(\partial\bar{\Lambda}_\alpha/\bar{x}_1)b_1/(2\bar{\Lambda}_\phi)$$

$$b_7=-b_3/\bar{x}_2-[(\partial\bar{\Lambda}_\alpha/\partial\bar{x}_1)b_2+(\partial\Lambda_\alpha/\partial\bar{x}_2)b_3]/(\bar{\Lambda}_\phi+\bar{\Lambda}_\alpha)$$

$$\partial\bar{\Lambda}_\phi/\partial\bar{x}_1=-[A/B+A/C-2]\bar{x}_1/[2\sqrt{1-\bar{x}_1^2}]$$

$$\partial\Lambda_\phi/\partial\bar{x}_2=1$$

$$\partial\bar{\Lambda}_\alpha/\partial\bar{x}_1=-\bar{x}_1/\sqrt{1-\bar{x}_1^2}$$

$$\partial\bar{\Lambda}_\alpha/\partial\bar{x}_2=-(1+A/B_1)$$

The procedure for obtaining Eqs. (32) is very straightforward. First, the parts of Eqs. (26) which are periodic in y_2 and y_1+y_2 are subtracted off. Then, $a \equiv x_1$, $p_\alpha \equiv x_2$, and $y_1 \equiv \phi - \alpha$ are replaced by $\bar{x}_1$, $\bar{x}_2$, and $\bar{y}_1$ to obtain the vectors U_1 and V_1 (see Appendix).

The process of obtaining Eqs. (33) is more complicated, but not so much as it first might appear. The procedure is basically as follows. First, the parts of Eqs. (26a) and (26c) which were subtracted off in obtaining Eqs. (32) are recovered. These form the vector $X_1(x, y)$ (see Appendix). The right-hand sides of Eqs. (32a) and (32b) form the vector U_1. The vector $X_1(\bar{x}, \bar{y}) - U_1$ then is formed, and the substitutions $\bar{y}_1 + \bar{y}_2 \equiv -2\bar{\Lambda}_\phi t^*$ and $y_2 \equiv -(\bar{\Lambda}_\phi + \bar{\Lambda}_\alpha)t^*$, where t^* is an auxiliary variable, are made. The vector P_1 defined by Eq. (A5a) then is obtained by integrating with respect to t^* and then replacing t^* by using the preceding substitutions. The vector Q_1 defined by (A5b) is obtained in a similar manner, using the right-hand sides of Eqs. (26b) and (26d), the partial derivative of $V_0 = (-\bar{\Lambda}_\phi \ -\bar{\Lambda}_\alpha)^T$ with respect to $\bar{x} = (\bar{x}_1 \ \bar{x}_2)^T$, and the previously obtained vector P_1.

Integrals and Geometrical Results

Although considerably simpler than Eqs. (26), Eqs. (32) are still rather formidable if $\bar{T}_\alpha \neq 0$. We can, however, obtain a first integral for the case $\bar{T}_\alpha = \text{const}$. Noting that $d(1-\bar{x}_1'^2)^{1/2}/d\tau = -\bar{x}_1\bar{x}_1'/(1-\bar{x}_1'^2)^{1/2}$, we obtain from Eq. (32a) the equation

$$\frac{d}{d\tau}\sqrt{1-\bar{x}_1'^2} = -\epsilon\mu\bar{x}_1\bar{x}_2[A/2C]\sin\bar{y}_1 \tag{34}$$

Hence, using Eqs. (32b) and (34) with $\bar{T}_\alpha$ constant, we get

$$\sqrt{1-\bar{x}_1'^2} + \bar{x}_2 = (\bar{T}_\alpha/H)t + C^* \tag{35}$$

where C^* is a constant of integration. Note that t, and not τ, appears in Eq. (35). Equation (35) represents a family of circles, each of unit radius with centers at $[0, C^* + (\bar{T}_\alpha/H)t]$. For $\bar{T}_\alpha < 0$, the centers of these circles approach the origin of the $\bar{x}_1\bar{x}_2$ plane as time t increases. Because the torque T_α typically will be small in magnitude, say 2 ft-lb, whereas H will be large, say around 2000 ft-lb-sec, the right-hand side of Eq. (35) will vary, at most, very slowly with time.

To proceed further toward an analytical solution, we put $\bar{T}_\alpha = 0$. Then, in addition to the integral $(1-\bar{x}_1'^2)^{1/2} + \bar{x}_2 = C^*$, we have an "energy" integral, since the averaged kinetic energy $\bar{\mathfrak{I}}$ is constant. By introducing the notation

$$L_1 \equiv \sqrt{1-\bar{x}_1'^2} = \cos\theta \tag{36a}$$

$$L_2 \equiv \bar{x}_1 \sin\bar{y}_1 = \sqrt{1-L_1^2}\sin\bar{y}_1 = \overline{\sin\theta}\,\sin\bar{y}_1 \tag{36b}$$

$$L_3 \equiv \bar{x}_1 \cos\bar{y}_1 = \sqrt{1-L_1^2}\cos\bar{y}_1 = \overline{\sin\theta}\,\cos\bar{y}_1 \tag{36c}$$

we may express this integral in the form

$$L_3 = (d_0 + d_1L_1 + d_2L_1^2)/[\mu\epsilon(C^* - L_1)/C] \tag{37}$$

where

$$d_0 = C^*[1/A + 1/B_1] - 2\mathcal{K}/A \tag{38a}$$

$$d_1 = -C^*[4/A + 2/B_1] \tag{38b}$$

$$d_2 = 4/A - (B+C)/(2BC) + 1/B_1 \tag{38c}$$

where $\mathcal{K}$ is a second constant of integration‡‡ which may be obtained from

$$\mathcal{K} = \tfrac{1}{2}\{\tfrac{1}{2}[(C-A)/C + (B-A)/B]L_1^2 - 2L_1\bar{x}_2 + (A/B_1+1)\bar{x}_2^2 - 2\mu\epsilon[A/(2C)]\bar{x}_2\sqrt{1-L_1^2}\cos\bar{y}_1\} \tag{38d}$$

by inserting values of L_1, $\bar{x}_2$, and $\bar{y}_1$ at any time.

The variables L_1, L_2, and L_3 may be interpreted physically as the averaged ξ, η, and ζ components of the rotational angular momentum of the spacecraft, where the $C\xi\eta\zeta$ coordinate frame is obtained from the $Cxyz$ frame by a negative rotation through α about the x axis (see Fig. 2). Near resonance, the $C\xi\eta\zeta$ frame rotates very slowly about its ξ axis while that axis precesses and nutates.

The integral (37) can be interpreted geometrically as a family of surfaces in the (L_1, L_2, L_3) space. Were the denominator of Eq. (37) constant, the surfaces would be parabolic cylinders.[10] However, because of factor $(C^* - L_1)$ in the denominator, the surfaces are such that for $L_1 \ll C^*$ they resemble parabolic cylinders, but they are asymptotic to the plane $L_1 = C^*$ and resemble planes for $L_1 \gg C^*$. An example of the projection of such a surface onto the L_1L_3 plane is shown in Fig. 6. The scale of the figure was adjusted to show the part of the projection of interest. The projection for $L_1 > C^*$ is not of interest because $C^* \geq 1$.

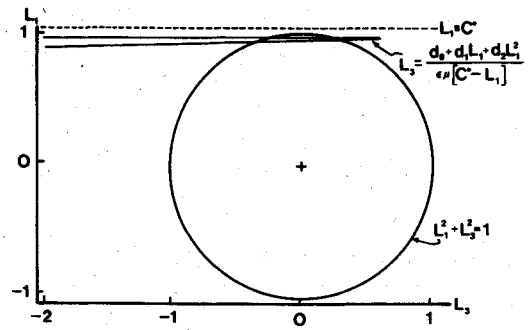

Fig. 6 Integrals of the motion.

The L_j also satisfy the condition

$$L_1^2 + L_2^2 + L_3^2 = 1 \tag{39}$$

Equation (39), of course, represents a unit sphere in the (L_1, L_2, L_3) space with center at the origin. It follows from Eqs. (37) and (39) that the L_j vary in such a way that the terminus of a vector L with components L_1, L_2, and L_3 traces out a curve of intersection of the sphere (39) and one of the family of surfaces defined by Eq. (37). Notice that, in general, a projection of $L_3 = f(L_1)$, as defined by Eq. (37), onto the L_1L_3 plane and the circle $L_1^2 + L_3^2 = 1$ may 1) intersect at two points, 2) intersect at four points, 3) intersect at two points and be tangent at a third point, 4) be tangent at a single point (see Fig. 7), or 5) not intersect at all nor be tangent. If there are only two points of intersection and no points of tangency, then there may be either motion in a single "mode" in which L_1 is periodic and $\bar{y}_1$ is monotonic (circulation), or motion in which $\bar{y}_1$ is bounded (libration) and never zero. If there are four points of intersection, then either of two "modes" of circulation-type motion is possible, with one mode exhibiting much more pronounced amplitude variations in L_1 than the other. Recalling that $L_1 = \overline{\cos\theta} = H_1/H$ and that $\omega_1 = (H_1 - P_\alpha)/A$, we would expect that these two types of motion would be observable in ω_1. Such is the case.[4]

If there are two points of intersection and a point of tangency, the motion is one of limitation, whereas a single point of tangency implies that an equilibrium state exists. Finally, the case of no intersection or tangency corresponds to "imaginary" motion, which, although mathematically possible, is not of interest physically.

‡‡As a point of interest, if we put $p_1 = L_1$, $p_2 = \bar{x}_2$, $q_1 = \bar{\Phi}$, $q_2 = \bar{\alpha}$, and $\bar{y}_1 = q_1 - q_2$ in Eq. (38d), we have the Hamiltonian for the averaged motion.

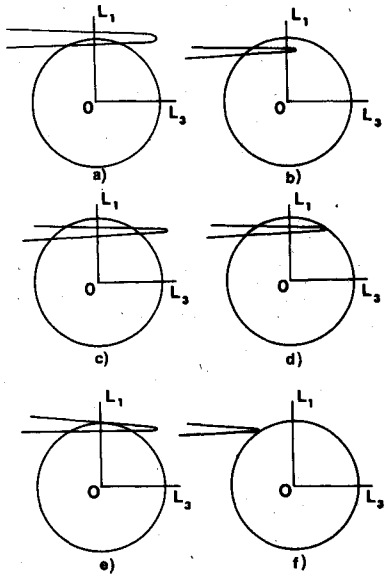

Fig. 7 Geometric interpretation of all possible long-term motions.

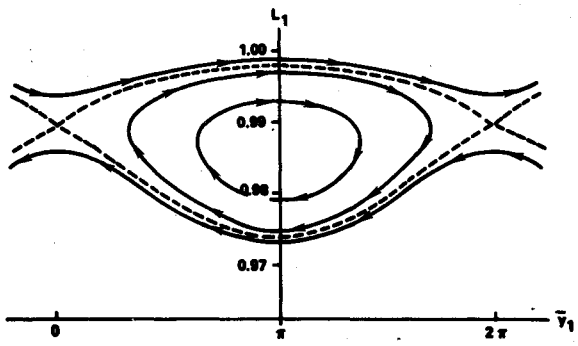

Fig. 8 L_1-$\bar{y}_1$ phase plane.

Equation (37) also may be used to study the motion in the $(L_1,\bar{y}_1)$ phase space, since

$$\cos\bar{y}_1 = (d_0+d_1L_1+d_2L_1^2)/[\epsilon\mu(C^*-L_1)\sqrt{1-L_1^2}] \qquad (40)$$

Some example phase plane curves, obtained using the data of Ref. 4, are shown in Fig. 8.

Solutions for $L_1(\tau)$ when $\bar{T}_\alpha = 0$

From Eqs. (34-36) for $\bar{T}_\alpha = 0$, we find that

$$dL_1/d\tau = [\epsilon\mu(C^*-L_1)A/(2C)]L_2 \qquad (41)$$

Then, by using the two integrals for the case $\bar{T}_\alpha = 0$, we obtain

$$\left[\frac{dL_1}{d\tau}\right]^2 = P(L_1) = a_4L_1^4+a_3L_1^3+a_2L_1^2+a_1L_1+a_0 \qquad (42)$$

where

$$a_4 = -[(\mu\epsilon A/C)^2+d_2^2]/4$$

$$a_3 = [(\mu\epsilon A/C)^2C^*-d_1d_2]/2$$

$$a_2 = [(\mu\epsilon A/C)^2(1-C^{*2})-2d_0d_2-d_1^2]/4$$

$$a_1 = -[(\mu\epsilon A/C)^2C^*+d_0d_1]/2$$

$$a_0 = [(\mu\epsilon A/C)^2C^{*2}-d_0^2]/4$$

Thus, $dL_1/d\tau$ is the square root of a quartic in L_1. It follows, from the theory of elliptic integrals,[11] that L_1 may be expressed as a function of Jacobian elliptic functions of $\tau=(H/A)t$.

Now, the roots of the quartic equation, $P(L_1)=0$, are roots of $L_2^2=0$, because $C^*\geq 1$ and $L_1<1$ for the motion considered here. Furthermore, roots of $L_2^2=0$ are the values of L_1 at the intersections of the projections of the integrals (37) and (39) onto the L_1L_3 plane.

The solutions to Eq. (41) for the first four of the cases noted previously may be obtained by using tables of elliptic integrals, for example, the extensive ones of Ref. 11. In general, the solution for L_1 is either of the form

$$L_1 = \frac{F_1+F_2\,\mathrm{sn}^2u}{F_3+F_4\,\mathrm{sn}^2u} \quad \text{(four unique real roots)} \qquad (43)$$

or the form

$$L_1 = \frac{G_1+G_2\,\mathrm{cn}\,u}{G_3+G_4\,\mathrm{cn}\,u} \quad \text{(two unique real roots and two complex roots)} \qquad (44)$$

where the F_j and the G_j are constant. Also, $u=\lambda(\tau-\tau_0)$, where λ and τ_0 are constant. In the special case (shown in Fig. 7e) where the particular surface of the family defined by Eq. (37) is tangent at the "top" of the sphere and intersects the sphere twice for smaller values of L_1 and motion takes place on the "lower" curve of intersection, the solution reduces to trigonometric functions. Also, in the case (Fig. 7d) where the particular surface of the family defined by Eq. (37) intersects the sphere at two values of L_1, say L_{11} and L_{12}, and is tangent to the sphere for a value of L_1 between L_{11} and L_{12}, the solution reduces to hyperbolic functions and is one of limitation,[12] for example, the motion corresponding to the separatrix of Fig. 8. A single point of tangency corresponds to a stable equilibrium, for example, the libration center in Fig. 8.

The task of obtaining explicit analytical solutions for the motion of the spacecraft relative to the angular momentum frame $CXYZ$ is relatively straightforward, but the details have not been worked out to date. However, it may be concluded that the angles $\bar{y}_1$ and $\bar{y}_2$ probably can be expressed in terms of Jacobian elliptic functions and elliptic integrals of the second and third kinds. The effort required to do this probably is not warranted, however, since the essence of the motion is embodied in the integrals already obtained.

Some Quantitative Results for the $\bar{T}_\alpha = 0$ Case

The period of the motion in L_1 may be determined for any particular case, once the roots of the quartic equation $P(L_1)=0$ are known. For the case of four, real, distinct roots z_j, $j=1,2,3,4$, where $z_1>z_2>z_3>z_4$, this period (in seconds) is $T=2K/(\lambda H/A)$, where K is the complete elliptic integral of the first kind of modulus

$$k=\sqrt{[(z_1-z_2)(z_3-z_4)]/[(z_1-z_3)(z_2-z_4)]}$$

and

$$\lambda = \tfrac{1}{2}\sqrt{|a_4|}\,\sqrt{(z_1-z_3)(z_2-z_4)}$$

As an example of the accuracy of the approximate solution, we consider the conditions $L_1=0.9890$, $\bar{x}_2=0.1056$, and $\bar{y}_1=0$, which correspond to the zero net motor torque results of Ref. 4. These conditions were used along with $H=1800$ slug-ft^2/sec and the previously stated values of A, B_1, C, B_1, and P, and the roots of $P(L_1)=0$ were calculated. Explicitly, it was found that $z_1\simeq 0.9968$, $z_2\simeq 0.9896$, $z_3\simeq 0.9861$ and $z_4\simeq 0.9712$. The modulus for this particular case is $k=0.7381$. The corresponding value of K (from the appropriate table in Ref. 11) is 1.894 and $\lambda\simeq 0.02204$. The

period is therefore approximately 28.64 sec. According to Ref. 4, the period of the long-period, or "low-frequency," motion in ϕ and ω_1 for this case is approximately 22.44 sec.

For the data just cited, the maximum and minimum values of the "average" coning angle may be computed by using $\bar{\theta} \equiv \cos^{-1}(L_1)$. For the "primarily nutation mode" of Ref. 4, $\bar{\theta}_{min} \simeq 4.58°$ and $\bar{\theta}_{max} \simeq 8.27°$; whereas, for the "primarily low-frequency mode," $\bar{\theta}_{min} \simeq 9.56°$ and $\bar{\theta}_{max} \simeq 13.78°$.

On the basis of the theory presented here, the frequency of the high-frequency mode, noted in Ref. 4 to be 3.4 rad/sec, should be approximately $H(\bar{\Lambda}_\alpha + \bar{\Lambda}_\phi)/A$ or, since $\bar{\Lambda}_\phi \simeq \bar{\Lambda}_\alpha$ near resonance, $2H\bar{\Lambda}_\phi/A$. Because $\bar{\Lambda}_\phi$ is not constant, we shall consider the values of $\bar{\Lambda}_\phi$ corresponding to maximum and minimum values of L_1 for the "low-frequency mode." Since $L_1 + \bar{x}_2 = C^*$,

$$\bar{\Lambda}_\phi = \tfrac{1}{2}[A/C + A/B - 4]L_1 + C^*$$

For this example, $C^* \simeq 1.089$, and the two values are 2.85 and 3.11 rad/sec. The discrepancy in these results is probably due to the relatively large value of ϵ (i.e., 0.4) dictated by the data.

Effects of Nonzero $\bar{T}_\alpha$

If $\bar{T}_\alpha$ is a negative constant, then $C^{**} = C^* + (\bar{T}_\alpha/H)t$ decreases as t increases. As $C^{**} \to 1$, $(1 - \bar{x}_1^2)^{1/2} \to 1 - \bar{x}_2$. Also, it can be shown that the energy increases with time if $\bar{T}_\alpha < 0$ and $\dot{\alpha} < 0$. As the energy increases, so does $\mathcal{K}$. Furthermore, if the torque were removed at any instant of time, the integrals (35) and (37) would be valid. Their instantaneous, or osculating, forms then allow us to describe the motion, except for the phase. That is, the parabolic surface and sphere together determine the possible loci of the terminus of vector $L = (L_1\ L_2\ L_3)^T$ but do not determine where on the loci it is at a given time.

Equations (32) were integrated numerically with $\bar{T}_\alpha = -1.25$ ft-lb, and "parabolic" surfaces corresponding to different instants of time were determined. It was found that, as the time increases, the top of the "parabolic" surface is "pushed down" while the maximum value of L_3 decreases for a time and then increases. This sequence is depicted in Fig. 9. Figure 9a shows that initially only one curve of intersection exists. As time increases (Fig. 9b), the once almost circular curve of intersection acquires a "clown's mouth" shape. "Resonance," that is, $\bar{\Lambda}_\alpha = \bar{\Lambda}_\phi$,§§ takes place at the points indicated by r's. As time increases further (Fig. 9c), the maximum value of L_3 starts increasing, the "parabolic" surface pierces the sphere, and two curves of intersection are formed. Whether the spacecraft is in a "resonance trap" at this point depends upon which of the curves of intersection correspond to the actual motion. If the motion is along the bottom curve, the spacecraft is trapped. However, if the motion follows the top curve, the resonance trap has been avoided. Thus, theoretically, the resonance trap may be avoided by properly timing the instant when the two curves of intersection first appear. Also, if the spacecraft becomes trapped, by reversing the torque a single curve of intersection can be achieved, and, by turning on negative torque only while the top part of the curve is being transversed, escape from the trap should be possible. Since $d\bar{y}_1/d\tau$ is positive for at least part of the time that the top part of the curve is being transversed, the sign of $d\bar{y}_1/d\tau$ possibly could be used as a switching function.

The integral (35) gives an indication of why the resonance trap results in increasingly large coning angles. It implies that, for a negative $\bar{T}_\alpha$, $\bar{x}_2$ may decrease and $(1 - \bar{x}_1^2)^{1/2} = \cos\bar{\theta}$ may stay fairly constant. This is the desired result. However, there is also the possibility that $\bar{x}_2$ will remain fairly constant while $\cos\bar{\theta}$ decreases. This is the resonance trap case.

§§Note: $\bar{\Lambda}_\alpha = \bar{\Lambda}_\alpha(\bar{x}_1, \bar{x}_2)$ and $\bar{\Lambda}_\phi = \Lambda_\phi(\bar{x}_1, \bar{x}_2)$.

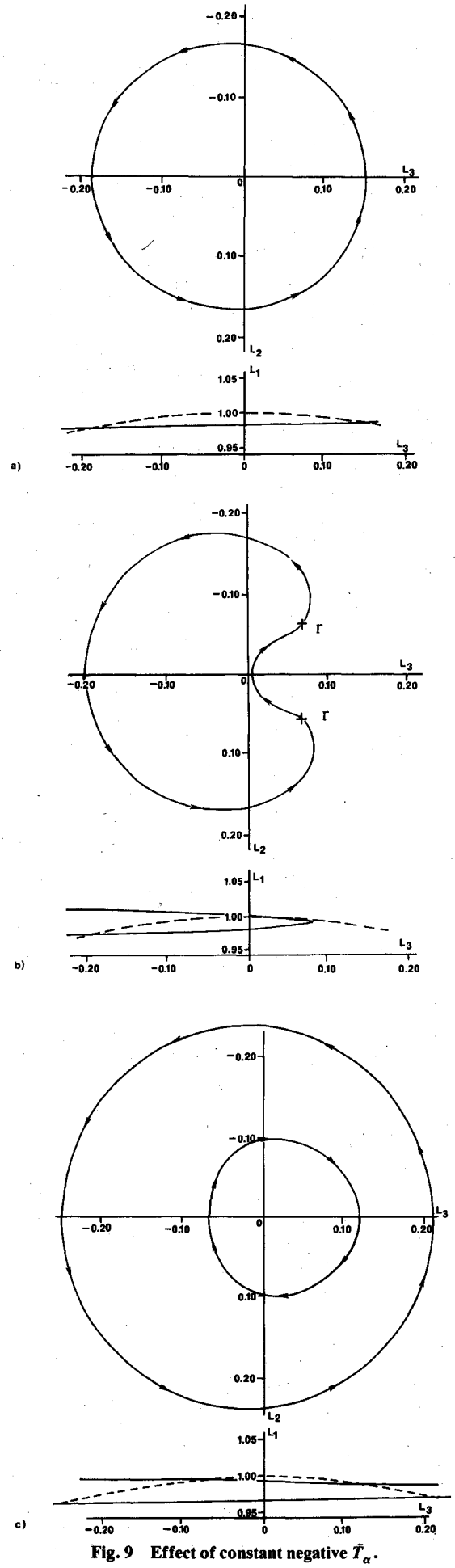

Fig. 9 Effect of constant negative $\bar{T}_\alpha$.

Avoiding and Escaping from the Resonance Trap

There are several ways of avoiding a resonance trap of the type studied here besides building a perfect spacecraft. The most obvious is to provide a great deal of torque and thereby render the periodic parts of the equation for P_α insignificant compared to the torque. An estimate of the torque required may be obtained using Eq. (32b). By requiring that $|A\bar{T}_\alpha/H^2|$ be larger than the amplitude of the periodic part, we find that if

$$|\bar{T}_\alpha| > |\epsilon\mu H\bar{x}_{1_{\max}}\bar{P}_{\alpha_{\max}}/(2C)| \tag{45}$$

no problem should arise. Using the inertia data on Ref. 4 and also $H\bar{x}_{1_{\max}} = 550$ ft-lb-sec and $\bar{P}_{\alpha_{\max}} = 200$ ft-lb-sec, we find that $T_\alpha > 8$ ft-lb should be sufficient. Since the required torque is proportional to the product $\mu\epsilon$, decreasing either μ or ϵ, or both, would allow for transversal of the resonance trap with a smaller-magnitude torque.

Another way to avoid resonance is to design the spacecraft such that $A > 4BC/(B+C)$. Then $\gamma < 1$, and there will be no resonance during despin. This may not, as Fig. 4 indicates, be practical. Finally, the method used in Ref. 4 to escape from the resonance trap may be used. The method used in Ref. 4 can be interpreted in light of the theory developed here. There escape was achieved by switching the motor off as "resonance" was approached. Large-amplitude motion, corresponding to the case in which there are only two intersection points (see Fig. 7b or 9b), occurred, since the kinetic energy was decreased by the action of the fractional torque. The motor was turned on during the last half "cycle" of the long-period, or low-frequency, oscillation in the nutation angle. This corresponded to turning the torque on between the two maximum values of L_3 (see Fig. 9b) when θ is smaller. That is, the motor was turned on while motion in θ corresponding to the top part of the "parabolic" surface was occurring. It then was turned off during the rest of the "cycle" and on again when the top of a new, higher-energy (more energy was put in by the motor than was expended overcoming friction) "parabolic" surface was being transversed. Penetration of the sphere by the "parabolic" surface occurred during the time when the top half of the "parabolic" surface was being transversed, and motion corresponding to, for example, the small curve in Fig. 9c was obtained. Escape thus was achieved by properly "timing" the application of torque.

VII. Conclusion

In despinning the platform of a dual-spin spacecraft that consists of a slightly asymmetric rigid rotor and a platform that has two equal moments of inertia about axes transverse to the spacecraft's bearing axis but is dynamically unbalanced with respect to the bearing axis, a resonance trap may be encountered. We have shown analytically that the occurrence of such a phenomenon requires both triaxiality of the rotor and dynamic unbalance of the platform. In addition, the inertia characteristics of the rotor and platform must be such that $A < 4BC/(B+C)$, or the condition for resonance will not be satisfied during despin. The attitude motions (excepting precession) of such a spacecraft have been studied geometrically and analytically, and the salient characteristics of the long-period motion near resonance, including the resonance trap state, have been described. Analytically derived results have been presented which agree qualitatively, and to some extent quantitatively, with the numerical results of Scher and Farrenkopf[4] even though the "small" parameter, $\epsilon = P/B_1$, in the analytical solution is not very small.

Several ways of avoiding or escaping from the resonance trap have been discussed. The construction of a spacecraft such that $A > 4BC/(B+C)$ and, hence, $\gamma < 1$, does not appear to be a practical way to avoid resonance if $2(B_2+D)/B$ is greater than about 0.05, because, in order to satisfy the criteria insuring $\gamma < 1$ and $A > B$ and C, it indicates that a very asymmetric rotor should be used. Another alternative is to provide sufficient motor torque. An expression for estimating the magnitude of the torque required has been presented [see Eq. (45)]. This expression indicates that, for a given motor, in-orbit mass balancing of some type might be used to make μ sufficiently small, or the platform could (if possible) be rotated about one of its transverse axes to make ϵ sufficiently small. Finally, there is the switching method of Ref. 4.

Appendix: Method of Averaging Algorithm

Algorithms for the method of averaging are given in many places[1,6-8] in the literature on nonlinear oscillations. The one presented here is given merely as a convenience to the reader. Given a system of nonlinear, ordinary differential equations of the form

$$\dot{x} = \delta X_1(x,y) + \delta^2 X_2(x,y) + \ldots \tag{A1a}$$

$$\dot{y} = Y_0(x) + \delta Y_1(x,y) + \delta^2 Y_2(x,y) + \ldots \tag{A1b}$$

where x is an M vector, y is an N vector, and X_j and Y_j are smooth functions of the elements of x and y and are periodic with period 2π in the elements of y, and δ is a "small" constant, an approximate solution to the system which is valid through first order in δ may be obtained by solving the "averaged" equations:

$$\dot{\bar{x}} = \delta U_1(\bar{x}) + \delta^2 U_2(\bar{x},\bar{y},\delta) \tag{A2a}$$

$$\dot{\bar{y}} = V_0(\bar{x}) + \delta V_1(\bar{x}) + \delta^2 V_2(\bar{x},\bar{y},\delta) \tag{A2b}$$

Here

$$V_0 = Y_0(\bar{x}) \tag{A3a}$$

$$U_1 = \frac{1}{(2\pi)^N}\int_0^{2\pi}\cdots\int_0^{2\pi} X_1(\bar{x},\bar{y})\,d\bar{y}_1\cdots d\bar{y}_N \tag{A3b}$$

$$V_1 = \frac{1}{(2\pi)^N}\int_0^{2\pi}\cdots\int_0^{2\pi} Y_1(\bar{x},\bar{y})d\bar{y}_1\cdots d\bar{y}_N \tag{A3c}$$

and the "averaged" variables $\bar{x}$ and $\bar{y}$ are related to the original variables by

$$x = \bar{x} + \delta P_1(\bar{x},\bar{y}) \tag{A4a}$$

$$y = \bar{y} + \delta Q_1(\bar{x},\bar{y}) \tag{A4b}$$

In Eqs. (A4), P_1 and Q_1 are solutions of the partial differential equations

$$\frac{\partial P_1}{\partial \bar{y}} V_0 = X_1(\bar{x},\bar{y}) - U_1 \tag{A5a}$$

$$\frac{\partial Q_1}{\partial \bar{y}} V_0 = Y_1(\bar{x},\bar{y}) - V_1 + \frac{\partial V_0}{\partial \bar{x}} P_1 \tag{A5b}$$

Acknowledgments

Part of the research reported herein was conducted while the author was a Visiting Associate Professor of Aerospace Engineering in the Department of Engineering Science and Systems of the University of Virginia. Additional support was provided by the Auburn University Engineering Experiment Station. Much of the programming involved in obtaining numerical results was performed by James R. Beaty, Graduate Research Assistant, at Auburn University. Finally, several helpful comments of the reviewers are acknowledged.

References

[1] Kyner, W.T., "Lectures on Nonlinear Resonance," NASA PM-81, 1969, pp. 255-299.

[2] Hitzl, D.L. and Breakwell, J.V., "Resonant and Non-resonant Gravity-Gradient Perturbations of a Tumbling Tri-Axial Satellite," *Celestial Mechanics,* Vol. 3, April 1971, pp. 346-383.

[3] Pringle, R., Jr., "Satellite Vibration-Rotation Motions Studied Via Canonical Transformations," *Celestial Mechanics,* Vol. 7, June 1973, pp. 495-518.

[4] Scher, M.P. and Farrenkopf, R.L., "Dynamic Trap States of Dual Spin Spacecraft," *AIAA Journal,* Vol. 12, Dec. 1974, pp. 1721-1725.

[5] Cochran, J.E., "Application of Canonical Transformation Theory to a Nonconservative Astrodynamical System," *AAS/AIAA Astrodynamics Specialists Conference,* AAS Paper 71-346, Fort Lauderdale, Fla., Aug. 17-19, 1971.

[6] Morrision, J.A., "Generalized Method of Averaging and the Von Zeipel Method," *Methods in Astrodynamics and Celestial Mechanics,* edited by R.L. Duncombe and V.G. Szebehely, Academic Press, New York, 1966.

[7] Bogoliuboff, N.N. and Mitropolsky, Y.A., *Asymptotic Methods in the Theory of Nonlinear Oscillations,* Gordon and Breach, New York, 1961.

[8] Liu, J.J.F., "Satellite Motion about an Oblate Earth," *AIAA Journal,* Vol. 12, Nov. 1974, pp. 1511-1516.

[9] Leimanis, E., *The General Problem of the Motion of Coupled Rigid Bodies about a Fixed Point,* Springer-Verlag, New York, 1965, pp. 21-24.

[10] Cochran, J.E., "Effects of Gravity-Gradient Torque on the Rotational Motion of a Triaxial Satellite in a Precessing Elliptic Orbit," *Celestial Mechanics,* Vol. 6, Sept. 1972, pp. 127-150.

[11] Byrd, P.F. and Friedman, M.D. *Handbook of Elliptic Integrals for Engineers and Scientists,* 2nd rev. ed., Springer-Verlag, New York, 1971, pp. 95-98.

[12] Pars, L.A., *A Treatise on Analytical Dynamics,* Heinman, London, 1965, pp. 47-49.